Research Article

Per Lindh and Polina Lemenkova*

Shear bond and compressive strength of clay stabilised with lime/cement jet grouting and deep mixing: A case of Norvik, Nynäshamn

https://doi.org/10.1515/nleng-2022-0269
received September 1, 2022; accepted December 16, 2022

Abstract: The strength of soil can significantly increase by stabilisation with binders. Adding binders in correct proportions to improve soil parameters is of paramount importance for earthworks. In this article, we presented a framework to explore strength characteristics of soil stabilised by several binders and evaluated using applied geophysical methods by estimated P-wave velocities. The core of our work is a systematic assessment of the effects on clay stabilisation from various binders on shear and compressive strength. The binders were combined from four stabilising agents: (i) CEM II/A, a Portland limestone cement; (ii) burnt lime; (iii) lime kiln dust (LKD) limited up to 50%; and (iv) cement kiln dust (CKD). Shear strength has shown a nonlinear dependence as an exponential curve with P-waves. Natural frequency analysis was modelled to simulate resonant frequencies as eigen values. Variations in strength proved that CEM II/A-M (Recipe A, 100% CEM II) has the best performance for weak soil stabilisation followed by the combinations: Recipe B (70% CEM II/A-M, 30% LKD), Recipe C with added 80% CEM II/A-M and 20% CKD, and Recipe D (70% CEM II/A-M 30% CKD). Recipe B has shown high values with maximum uniaxial compressive strength (UCS) at 13.8 MPa. The Recipe C was less effective with the highest value of UCS as 8.8 MPa. The least strength was shown in Recipe D, where UCS has maximal values of 3.7 MPa. The specimens stabilised by Recipe B demonstrated the highest P-wave velocity at 2,350 m/s, while Recipe C and Recipe D showed the highest P-wave velocity at 1,900 and 1,550 m/s. All specimens shown a gain of UCS with sharply increased P-wave speed during the 3 days of curing. The study contributes to the development of methods of soil testing in civil engineering.

Keywords: civil engineering, foundation, soil stabilisation

PACS: 81.40.Cd, 81.40.Ef, 62.20.Qp, 83.50.Xa, 45.70.Mg, 92.40.Lg, 81.40.Lm, 62.20.M

*** Corresponding author: Polina Lemenkova,** Université Libre de Bruxelles (ULB), École polytechnique de Bruxelles (Brussels Faculty of Engineering), Laboratory of Image Synthesis and Analysis (LISA). Campus de Solbosch, ULB – LISA CP165/57, Av. F. D. Roosevelt 50, B-1050 Brussels, Belgium, e-mail: polina.lemenkova@ulb.be
Per Lindh: Swedish Transport Administration, Department of Investment, Box 366/ Neptunigatan 52, SE-201 23 Malmö, Sweden, e-mail: per.lindh@trafikverket.se, per.lindh@byggtek.lth.se

1 Introduction

1.1 Background

The mechanical performance of soil under load stress has a complex and nonlinear behaviour. This is largely controlled by a variety of inner and external factors responsible for soil formation [1–3]. The environmental factors such as temperature and humidity are determined by regional factors, and control the distribution of soil minerals [4,5]. Inner properties may vary according to the complex structure of soil as a porous media with varied mineral content, texture, density, porosity, viscosity, elasticity, compactness, and grain size [6,7].

The behaviour of weak soil presents a serious problem in earthworks and construction industry. Weak soils such as swelling clays pose a significant hazard to foundations for buildings due to the uplift pressures. Reparation works on buildings damaged by expansive soils can lead to serious financial costs reaching dozens, thousands of euros. Moreover, different types of dynamic loads may occur in foundations of structures including the effects of vibrations in buildings [8]. Special cases include the foundations under precast reinforced concrete columns of steel or flyovers and industrial structures used for transferring loads to the ground in the structural systems [9,10].

The analytical and design part for such constructors includes the selection of the appropriate technology of soil stabilisation and reinforcement of the foundation

before construction works on installation of industrial skeletons. Soil stabilised by binders gains in strength, which ensures its resistance to the external loads. Stabilised soils help to significantly reduce the effects of building exploitation and ensure the stability of constructions. The traditional binders include cement and cementitious materials [11], as well as other binders, such as slag [12], and fly ash [13,14].

Jet propagation in soil is performed from the injection nozzle, which results in cementation of soil due to the interaction of particles between the jet of binders and, soil. The injected fluid penetrates into the soil, increases pore pressures, and reduces grain contact in a soil skeleton [15,16]. This results in the increased stiffness, density, and strength of soil stabilised by jet grouting [17]. The jet grouting technique is a soil consolidation process based on grouting of fluid jet of cementitious slurry through a jet column into the ground [18]. Major parts of the jetting mechanism include the grout pipe connected to the drilling device, monitor, rod, and nozzle [19]. A borehole is drilled up to the targeted depth with cementitious slurry injected to the ground through a column and mixed with soil. The drill stem is then removed slowly from the borehole [20]. Originally developed in the United Kingdom, jet grouting has now been largely used for soil hardening in engineering works [21–23].

The advantages of jet grouting include a straightforward and effective implementation, economic benefits, and improved technological solutions for improving mechanical properties of soil [24]. Jet technology increases bearing capacity of soils and reduces settlements of foundations, which is the target goal in geotechnical works [25]. Technical, economic, and environmental advantages of jet grouting [26] made it useful in diverse applications in civil engineering including tunnelling [27], airports [28,29], and metro and subways [30–32]. The technical advantages of jet grouting include its flexibility [33] and applicability in all major types of soil: silt [34,35], clay [36,37], or sand [38].

Deep soil mixing technique is an *in situ* method of ground improvement, which is based on mechanical mixing of soil with cementitious binder [39,40]. By deep mixing, soils are blended systematically with cementitious binders using column technique using drilling and jet grouting [41,42]. Deep mixing involves the use of either wet or dry mixing techniques. While wet mixing injects slurry of cementitious binders, dry mixing uses powder binders that react with water in soil [43]. It is especially useful for the cohesive fine-grained type of soil, *e.g.*, clay [44,45], because soft and weak soil has a high moisture content and loose structure that can be stabilised using deep mixing [46]. Existing cases of deep soil mixing report increased shear modulus [47], reduced compressibility and improved parameters of the compressive strength [48], and reduced ground settlement and improved soil stability [49].

The strength characteristics of soil have a key role in construction, as they control the performance of ground in terms of service ability [50]. The effectiveness of soil stabilisation depends on many factors: soil type, stabilising agent, curing time and temperature, water content, and drainage conditions [51]. For geotechnical purpose, critical factors include the content of binder, water–binder ratio [52–54], and confining pressure [55–57]. Therefore, the effective methods of controlling soil strength are of paramount importance and great interest for civil engineering as practical solutions of geotechnical construction works. We have contributed to this issue by demonstrating the methods of evaluating soil strength adopted to a clay type of soil stabilised by four different binders and evaluated by P-wave velocities.

1.2 Related works

There is an increasing trend to explore material properties by geophysical methods applied for civil engineering domain, in particular using nonlinear wave analysis. Stress changes in materials can be evaluated through acoustic wave analyses using either–elastic acoustic waves [58] or coda-wave interferometry and nonlinear acoustic waves [59], which are sensitive to the microstructural changes in materials. The acoustic emission technique and the extraction of resonant frequencies can effectively be used for non-destructive dynamic testing of damage in cementitious structures [60]. The ultrasonic shear-horizontal waves can be applied for estimating cracks in the construction elements, which is of critical importance for evaluating the structural safety [61].

It is known that geophysical properties of P-wave velocity correlate with key engineering characteristics of the soil structure such as rigidity, compressibility, and density. In turn, these are related to a number of interrelated parameters of soil: viscosity, stiffness, compactness, and elasticity, which depends on density and porosity [62,63]. The velocity of P-wave at which it travels through a soil specimen can be measured using ultrasonic methods by accelerators, transducers, and receivers. Generally speaking, the velocity of the P-waves has strong positive

relationships with uniaxial compressive strength (UCS) [64,65]: the higher the strength of soil is, the higher is the P-wave velocity. Therefore, as curing time and binder content affect the soil strength, it can be used with regard to P-wave velocity as related parameters.

Shear and compressional wave velocities vary with different effective stress and porosity, which enables us to find a correlation between dominant frequency and inter-particle voids of soil [66]. With this regard, the investigation of the ultrasonic wavelength can be performed in various media, including compacted clay and sandy soil [67], fluid-saturated poroelastic soil [68], or in reinforced concrete structures [69,70] used in construction industry. One of these approaches is testing the shear bond and compressive strength of stabilised ground samples. Stabilising soil can be performed by a wide variety of binders, among which many applications use lime [71,72] and cement [73]. Lime–cement treatment is effective specifically for fine-grained type of soil: clay or silt [74–78].

The analysis of the performance of stabilised soil is a challenging task, since the addition of various combinations of binders may result in different responses from soil, depending on its structure and mineral content. For instance, the behaviour of fine-grained [79] or course-grained soil [80] differs, owing to the differences in mineral content and physico-chemical properties of soils [81]. As a result, different binders are needed for different types of soils [82,83]. Many solutions exist evaluating soil properties, each based on different techniques [84–88]. The universal methods for soil stabilisation do not exist and require laboratory testing and control for different types of soils and binders.

Testing shear bond and compressive strength of soil aims to estimate the parameters of soil performance under load regarding the content of binders and type of soil. This is primarily intended at evaluation of soil cementation upon stabilisation with various binders. It can be done either by pure binders or by blended mixtures with various components of stabilising agents [89,90]. The important physical parameters of the cementitious materials, affecting the performance of dynamically loaded reinforced concrete structures in civil engineering, include material elasticity, vibration energy absorption, dumping coefficient, and fatigue strength [91]. Hardening of the materials by binders enables us to improve strength parameters and increase the resistance to vibrations and resonance. Stabilised soil before construction of foundations gains sufficient impact resistance to dynamic loadings.

1.3 Study objectives

The Swedish Geotechnical Institute (SGI) has performed laboratory determinations and evaluation of strength properties on stabilised clay from Norvik, Nynäshamn municipality. The works have been carried out on behalf of the Geomind KB, SMA, and CEMEX. The research aim was to test different binder combinations for depth stabilisation and for jet grouting of clay. The tests included two types: (i) mixing tests for deep stabilisation and (ii) mixing tests for jet grouting.

This article focuses on the estimation of shear bond and compressive strength of clay collected in the Norvik, Nynäshamn Municipality, located in the central region of Sweden, Stockholm County. Soil of the cold regions is subjected to harsh environmental setting and has specific properties caused by ambient temperature below zero and repetitive seasonal freezing [92–95]. Such soil should be stabilised before the use in industrial works. The methods included stabilisation of specimens with lime/cement mixtures by deep mixing and jet grouting and seismic measurements of P-wave velocity.

2 Methodology

2.1 Binders

To evaluate binder combinations for deep stabilisation, an experimental setup of simplex centroid design was applied using existing methodology [96,97]. The purpose of using this type of statistical planning is to minimise the number of trials while maintaining the statistical significance and to ensure that both positive and negative interactions between the binder components are detected. Four different binders have been used in this study: (i) cement type CEM II/A, which is a Portland limestone cement consisting of Portland clinker (K) (content 80–94%) and limestone (LL); (ii) burnt lime (quicklime) named Ql in the figures (“quicklime”); (iii) lime kiln dust (LKD); and (iv) cement kiln dust (CKD). The effects from binders on soil stabilisation were evaluated by the nondestructive analytical techniques of seismic waves measurements.

The selection of binders is explained by the effectiveness of these stabilising agents on soil stabilisation, due to the mineral compositions. Thus, the compound composition of the ordinary portland cement (OPC) type II is as follows: according to the classification of the American

Society for Testing and Materials (ASTM), it consists of OPC up to 65% and up to 35% of other components. Due to the high percentage of Ca in its mineral content (dicalcium silicate (C_2S), tricalcium silicate (C_3S), and tricalcium aluminate (C_3A)), OPC is a powerful binder for stabilisation of clay, because each of these chemical compounds contributes and affects binding of particles through hardening process and soil stabilisation. For instance, C_3S is responsible for early strength development (reactions are reached by 28 days of soil curing), while C_2S ensures late strength development (after 28 days). Besides, OPC performs moderate sulphate resistance and emits less heat during hydration, which makes it practical for environmental engineering.

Quicklime is the base anhydride of $Ca(OH)_2$ (calcium hydroxide). Being a chemical derivative with high content of Ca, it is an effective and inexpensive chemical widely used in engineering construction works as a binder. It is widely used in soil stabilisation process to form cementitious strengthen products when reacting with soil particles. Quicklime contributes to the high degree of hydration process by $CaCO_3$ released into the soil–lime mixture, which ensures high strength in stabilised soil.

The CKD and LKD are the derivatives of cement and lime products. Their properties and behaviour in soil stabilisation are consistent with the chemical compositions of cement and lime. The LKD and CKD are important components for hydration reaction in a stabilised soil-binder mixture. Besides the type of binders, the increase in the compressive strength of soil-binder samples generally tends to gain over the period of curing and is affected by curing conditions: ambient air temperature, moisture, water content, and mineral composition of soil.

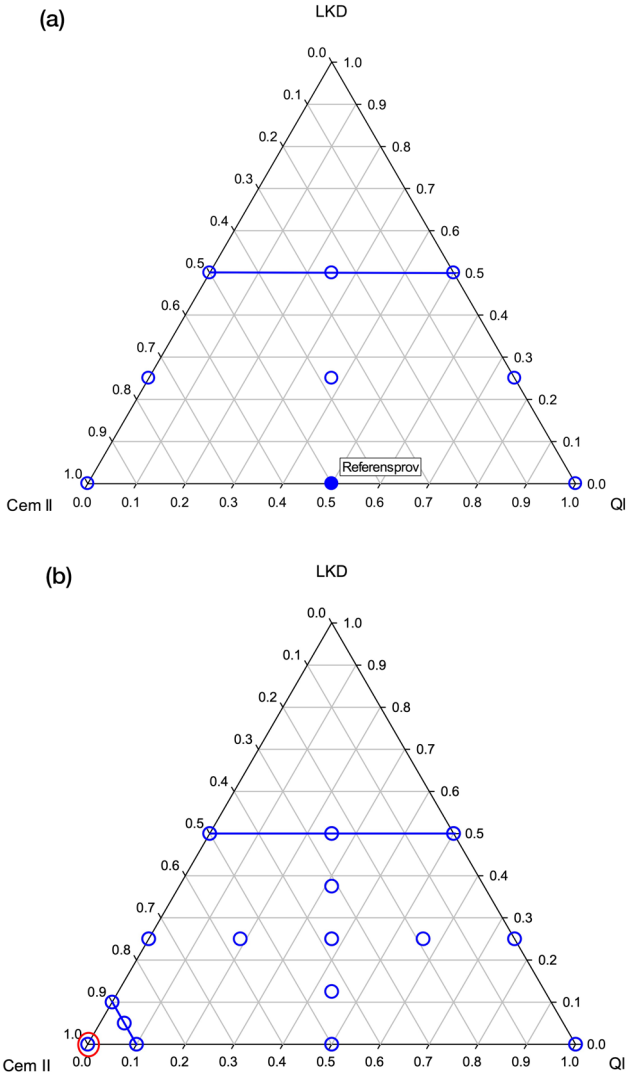

Figure 1: Experimental design: (a) according to a restricted simplex centroid design; (b) supplemented with internal points.

2.2 Simplex centroid design

The test surface in a three-factor simplex centroid design is structured as a triangle (Figure 1). Pure binders (100%) are represented as corners in a triangle and a mixture of the two to three binders along the triangle's stripes, as a combination of all the binders inside the triangle of the model. The selected trial points are marked as blue circles, which correspond to the tested binder combinations. The mutual ratio between the binders varies depending on the location of the test point within the triangle model. Thus, nine different binder combinations were formed from the mix of these three binders. The full circles represent both the test point and extra reference samples (Figure 1(a)).

The restricted simplex centroid design is shown in Figure 1(a), where the restriction consists in maximising the share of LKD to 50%. The test was used for the different amounts of binders: 80, 100, and 120 kg per m^3 of clay, respectively. The experimental design for the amount of binder 100 kg of binder per m^3 of clay was supplemented with the internal points, which increases the resolution of the response surface. Clay was added in various ratios in four recipes of various binders to evaluate the performance of soil with various clay content against binders (80, 100, and 120 kg per m^3 of clay). Red ring shows a point that were excluded from the analysis (Figure 1(b)). Each trial point was performed as a double trial with the corners of the triangle representing to the 100% of only one binder. The centre of the triangle corresponds to 33% of the three different binders. The points on the lower border of the triangle correspond to either a pure binder

(compared with CEM II/A or Ql) or, alternatively, to a mixture of 50% CEM II/A and 50% Ql.

The curing time for the reference samples (cement/lime 50/50) was determined to be 7, 14, 21, and 28 days. Extra reference tests have been carried out for calibration of seismic measurement in relation to the compressive strength on days 7 and 14 (Figure 1(b)). Moreover, some extra specimens were produced for the compression tests on day 80. The choice of 80 days is explained by the fact that the samples were stored at $T = 7\,°C$, which corresponds to the average ground temperature in central Sweden in the tested study area. At this storage temperature and a curing time of 80 days, this corresponds to the equivalent of 28 days of storage at 20 °C. The tests were carried out according to the laboratory guidance of the SGI applied in previous experiments [98,99] and existing methods of using lime/cement columns for deep column stabilisation [100].

2.3 Seismic measurements

Seismic measurements were performed as a free-free resonant column test measuring P-wave velocity of the specimen using existing methodology applied in previous studies [101,102]. The data were processed using software for seismic measurements, which records the P-wave speed from the obtained data and performs plotting (Figure 2).

The measurements were used on all specimens modelled in a previous step during simplex testing. Extra specimens were produced as reference specimens for the determination of P-wave velocity and shear strength on days 7 and 14. They present a reference to the P-wave velocity of the remaining specimens for a correlation to the shear strength of the samples. The correlation between the P-waves and UCS has previously been used for plotting response surface of the stabilised samples [103,104]. The velocity of the P waves in isotropic and homogeneous solids, such as soil, is given by the following formula:

$$\upsilon_p = \sqrt{\frac{K + \frac{4x}{3}\mu}{\rho}}, \tag{1}$$

where K is the bulk modulus (incompressibility), μ is the shear modulus (rigidity), and ρ is the density of soil through which the wave propagates [105]. From this equation, it is clear that P-wave velocity depends on the key material characteristics related to strength parameters – rigidity, compressibility, and density. The P-wave is the axial wave passing through the cylindrical specimen. The vibration was excited by a hammer that stroke on one end of the specimen and measured as P-waves by the accelerator device on another end, according to the workflow of the existing studies [106]. The P-wave has been correlated against the shear strength of the stabilised material. Coupling between the P-wave and the constrained modulus of the material M_x shows the elastic moduli, which describes the isotropic homogeneous materials, as represented by the following equation:

$$M_x = \rho_x V_P^2, \tag{2}$$

where V_P is the velocity of a P-wave and ρ is the density of soil specimen through which the elastic wave is propagating [107]. The specifics of these tests were that tested sleeves were not completely filled with the soil material. The empty sleeves had eigenfrequencies close to those of the test bodies. This meant that frequency in generated oscillation modes deviated significantly from the natural frequency of the samples located in sleeves. Since natural frequency of the sleeves was predominate, it was these frequencies that were measured, compared with Section 3.3. This meant that none of the measurements on the test

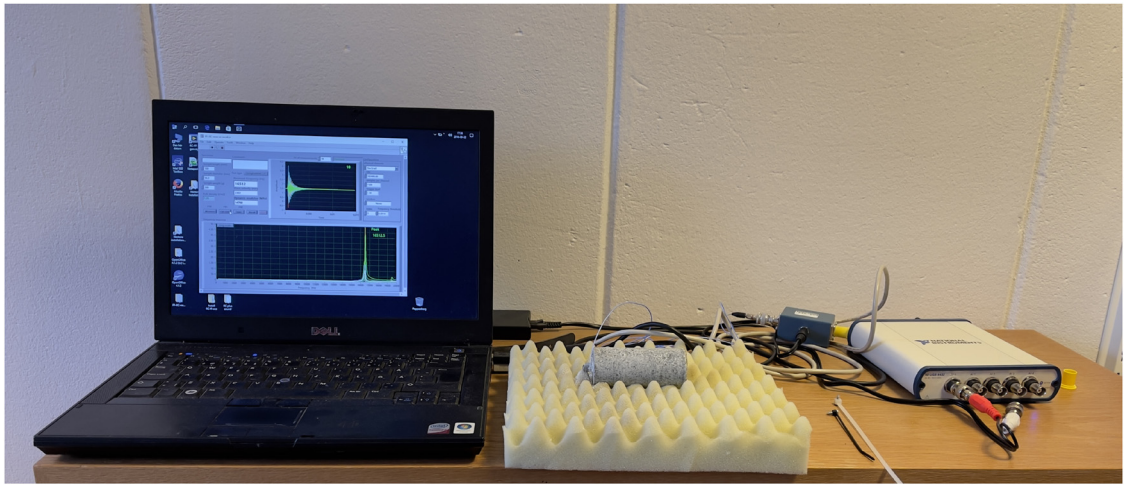

Figure 2: A process of seismic measurements which evaluates P-wave velocity of the specimen. Photo source: Per Lindh.

specimens in sleeves could be evaluated. In contrast, the tests performed on the deformed and trimmed specimens demonstrated the robust results.

2.4 Binder recipe for jet grouting

Testing of binder recipes has been carried out partly by the SGI and partly by the CEMEX. The surveys included the three types of tests: (i) UCS, (ii) water requirements, and (iii) binding time for the four types of soil-binder mixtures: (i) CEM II/A (100%); (ii) CEM II/A/CKD (50%/50%); (iii) CEM II/A/LKD (50%/50%); and (iv) CEM II/A/LKD/LSfiller (50%/30%/20%). The binder combinations were tested for the jet pillar grouting for reinforcement of soil, and summarised in Table 1, where J = performed test, and N = not performed test.

The tests carried out by the CEMEX comply with the Swedish standards of soil testing EN 196-1 [108] and EN 196-3 [109]. The conditions involve, among other parameters, that some binders have been mixed with the three parts of the standard sand and half a part water (vbt = 0.5). In the tests carried out at the SGI, only water and binder have been mixed, and in parts of the tests, clay has also been mixed in. This leads to significant differences in the compressive strength of the specimens. Furthermore, the test performed by the CEMEX is done on prisms, while the one in SGI is done on cylinders with a diameter of 50 mm and a height of 100 mm.

The binder and water were mixed by the industrial mixer for 5 min until a homogeneous mixture obtained as a technical equipment. The mixer is a stainless bowl with a capacity of about 5 L, which was fixed in the mixer frame during mixing, and a stainless steel blade with an axes driven by the electric motor. The process included mixing specimens with added binder and the predetermined amount of water, to obtain the required moisture. The samples were then cast into the test moulds. In cases where clay was added, mixing time increased to 20 min to obtain a homogeneous mixture. After 1–3 days of curing, the specimens were then de-shaped and trimmed to the correct length. Due to the water separation, the specimens were trimmed mostly on the upper part, because this part was weaker and could be processed more conveniently. There was no water separation in the tested samples containing clay. The testing was performed by CEMEX, and the proportion scheme is shown in Table 1. After the homogenising, mixing and compaction processes, the soil was stabilised and evaluated for strength.

Table 1: Tested binder combinations for the reinforcement of the jet grouting column. J = performed, N = not performed

Name	A	B	C	D
Cement (%)	100	70	80	70
LKD (%)	—	30	—	—
CKD (%)	—	—	20	30
vbt	1.0	1.0	1.2	1.2
Clay (17%)	J	J	J	N
Clay 30%	J	J	J	N
Clay 37.5%	J	J	J	N
Clay 58%	J	J	J	N

For jet grouting, cement (CEM II/A-M), LKD and CKD were used as binders and evaluated in terms of their performance. A water binder number (vbt) of 1.0 was used for binder in Recipes A and B, and a vbt of 1.2 was used for Recipes C and D, respectively. The experiments were carried out with the mixing of clay for the tested binder combinations.

The total clay content was 17, 30, 37.5, and 58% by weight. For binder Recipe D, no clay admixtures were carried out due to difficulties in obtaining a homogeneous admixture of clay in that sample and a low compressive strength without clay admixture. Tested binder ratios are reported in Table 1. Unlike the measurements performed on stabilised soil for lime/cement column reinforcement, all seismic tests were performed on the specimens without pipes. Furthermore, temperature measurements were carried out according to the thermos method on CEM II (100%) with a vct of 1.0 and CEM II/LKD (50/50%) with a vbt of 1.0. Steel thermoses with a liquid volume of 0.5 L were used for the experiment.

The viscosity was determined in Recipes A to D without added clay, according to the Marsh cone method. The Marsh cone is a workability test for quality control of cement grouts, which evaluates the fluidity based on the plastic viscosity and yield stress from the cone geometry of tested specimens [110]. It considers the rheological parameters and the time of flow in performance of soil-cement pastes, since plastic viscosity varies with composition of binders [111,112]. In this case, mixed clay recipes did not pass the funnel in the Marsh cone.

3 Results

3.1 Lime/cement column stabilisation

3.1.1 Strength determination

We evaluated the robustness of the interaction between lime, cement, CKD, and LKD on soil stabilisation. The

results demonstrated positive effects of binders on deep stabilisation of clay. Most of these binder combinations met the requirements for a minimum shear strength of soil at 200 kPa after 28 days of curing at 7 °C, that is, late strength development. The performed tests show that two of four tested recipes for jet grouting passed the requirement of 3 MPa after 28 days of curing even with a clay mixture of 58%. In the testing of binder combinations, a reference recipe of CEM II/A-V and quicklime were used in a mutual ratio of 50/50%. The evaluated shear strength for the reference samples at different curing times is reported in Figure 3.

To evaluate the effects from different binder combinations on shear bond and compressive strength of the stabilised material, a test was setup according to the simplex centroid design. The results are presented as a response surface for a binder quantity corresponding to 80, 100, and 120 kg/m^3 (Figure 4(a)–(c), respectively). Figure 4 provides example of the clear positive interaction between various components of stabilising agents (cement, quicklime, and LKD) in a binder combination. Positive interaction means that the components of binder taken together as blends generate a higher strength than would be expected from a linear regression between the effects of the single binders. The model achieved 95% of the explanation rate of variation in shear strength.

The results are comparable with those from the analysis of the extended trial reported in Figure 5, which shows a slightly lower positive interaction between the binders. Here, we performed the extended number of tests based on the effects from binders in the soil–binder mixture, which were setup for the amount of binder 100 kg/m^3 clay. In the trial set-up with more internal trial points, the resolution increases and the degree of explanation of the model increases from 95 to 97.5%. Figure 4 clearly demonstrate a generally increasing trend in gain of shear bond strength of all mixtures along with the added amount of binder.

Thus, the maximal values for 80 kg of binder show values over 200 kPa, for the binder bled of 100 kg – over 350 kPa, and for the binders of 120 kg of binder – over 450 kPa as maximal values (Figure 4). Thus, the LKD-Cem and Ql-LKD show relatively quick strength development along with the increased amount of binder (compared with 80, 100, and 120 kg of binder). Moreover, although the LKD-Cem mixture shows the highest strength and at all sample ages (corresponds to the bright red left corner of the triangle), the Ql-LKD mixture shows the lowest values (indicated by the green right corner of the triangle) (Figure 4).

The extended model shows a greater interaction between different binder components (Figure 5(a)). A 3D

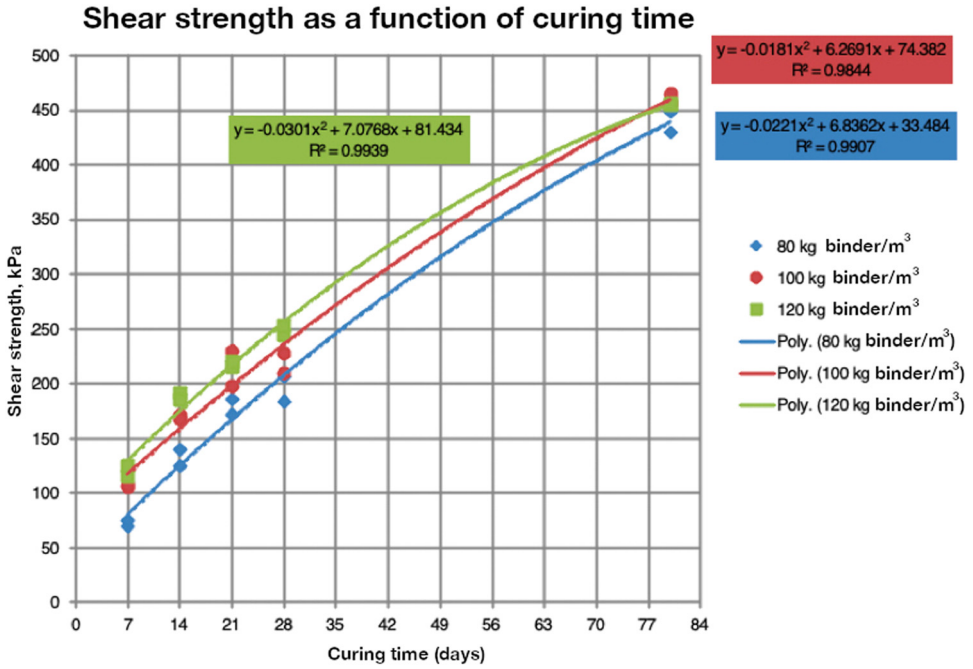

Figure 3: Shear strength as a function of curing time for specimens stabilised with a binder combination of CEM II/A and quicklime (50/50). The amounts of binder corresponded to 80, 100, and 120 kg of binder per m^3 of clay. The samples are stored in climate rooms with a temperature of 7 °C.

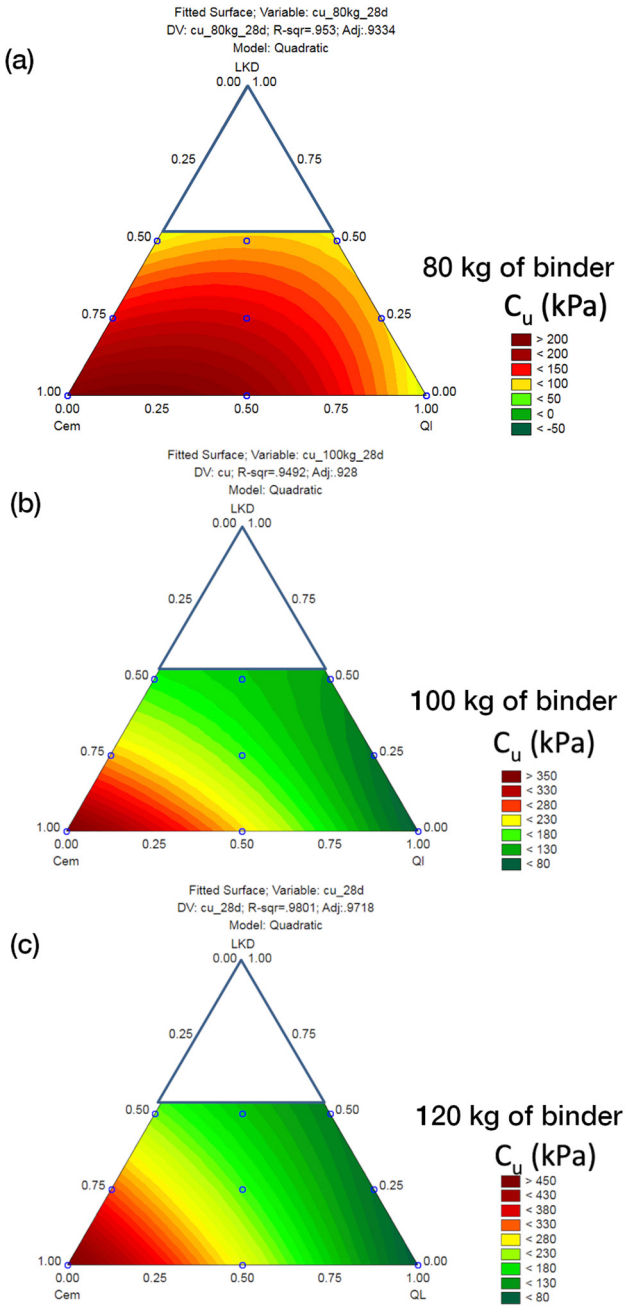

Figure 4: Response surface showing shear strength after 28 days of curing at 7 °C with varied amount of binders. (a) 80 kg/m^3, (b) 100 kg/m^3, (c) 120 kg/m^3.

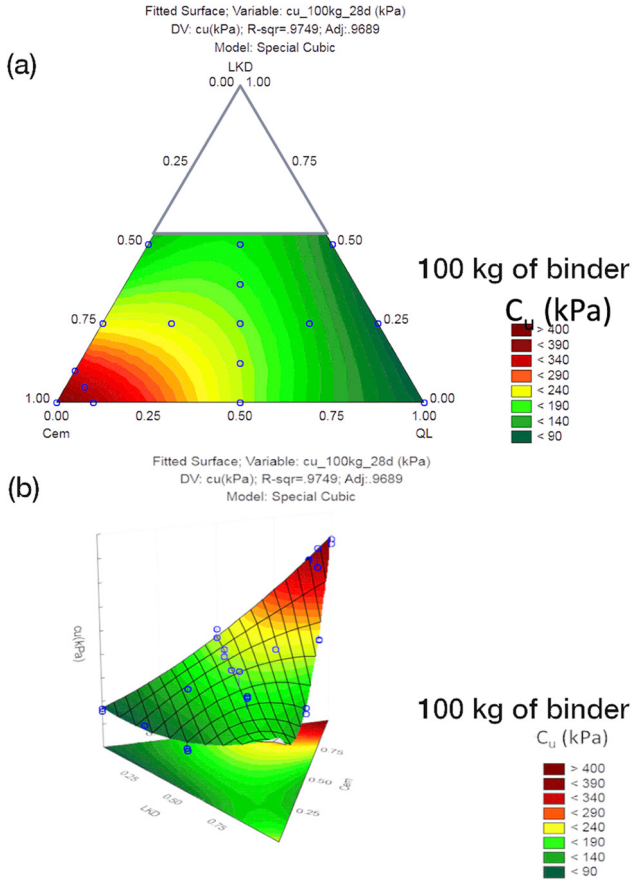

Figure 5: Response surface with internal points showing shear strength after 28 days of curing at 7 °C. The amount of binder 100 kg/m^3. (a) 2D view; (b) 3D view.

presentation of the ternary plots is generated in Figure 5(b) based on soil stabilisation data. It follows the response surface methodology that evaluates the correlation between the explanatory variables. These include binder components – cement, LKD, CKD, and quicklime, and the response variable (shear strength). In this mixture, the positive interaction of the binder components was rather small compared with the previous case. The degree of explanation of the response surface was 98%, which proves the robust results (Figure 5).

3.1.2 Seismic measurements

Seismic measurements were performed based on the evaluated velocity of the elastic P-waves, according to the free-free resonant column method. The shear strength of the material was considered for the dimensioning of lime/cement columns. This means that different binder recipes were assessed according to the recorded shear strength in soil specimens. The connection between the P-wave velocity and the UCS has a nonlinear form, which is largely dependent on the mineral composition of soil. The correlation between the P-wave velocity and shear strength of the stabilised soil is shown in Figure 6.

Figure 6 presents the results of the measurements of P-wave velocity and shear strength. The variations in binder ratio and composition were evaluated over the curing time of the experiments. There are also some

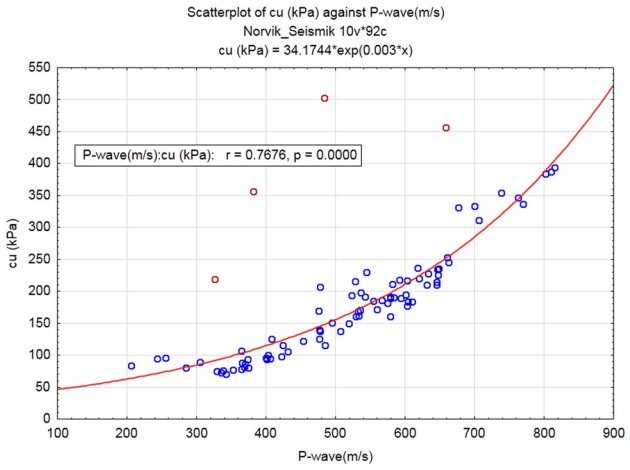

Figure 6: Shear strength as a function of P-wave velocity with red circles indicating identified outliers.

obvious outliers that have been identified and removed from the correlation plot (Figure 6). The results from the aforementioned measurements were used to estimate shear strength based on the measured P-wave velocity in the *in situ* conditions, *e.g.*, the crosshole measurements.

The analysis of the distribution of data values gives the following outcomes. The majority of data on shear strength is concentrated within the range of 65–250 kPa, which well corresponds to the P-wave velocity of 310–680 m/s. The increase in shear strength indicates the resistance of stabilised soil specimens to deformation by the effects from the tangential shear stress. In natural conditions, this also includes the resistance to erosion.

3.2 The effects of adhesives on jet grouted columns

To evaluate the effects from different binders on reinforcement of jet grouted columns, the tests of strength were carried out by CEMEX, according to the Swedish standard EN 196-1 (Figures 7 and 8). Binder, water, and a standard sand were used for testing [108]. In the other tests, we only used binders and water, and in some samples added a mixture of clay.

The results show that cement without the admixture of other binders gives the highest compressive strength, followed by a mixture of 50% CEM II and 50% LKD, and finally by a combination with 50% CEM II and 50% CKD, which gave a similar result to the combination of 50% CEM II and 30% LKD and 20% limestone filler. Figure 8 shows the UCS as a function of cement content for varied curing time. As demonstrated, the highest strength was

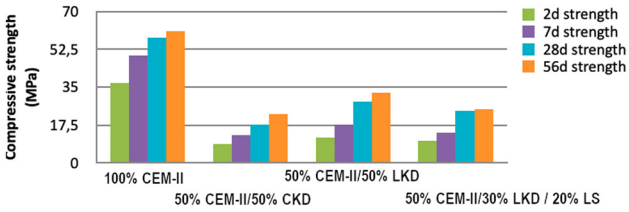

Figure 7: Compressive strength of specimens with different combinations of binders: cement (CEM II), CKD, LKD, and LS.

recorded for the pure CEM II followed by the mixture of 60% CEM II and 40% CKD. The mixture of 50% CEM II with 50% CKD demonstrated the lowest value of the compressive strength.

Figure 9 details setting time and water requirement for different binder combinations were investigated by CEMEX according to the Swedish standard EN 196-3 [109]. The compressive strength of tested four cases of binder ratios include the following mixtures (from left to right, Figure 9): (i) 100% cement (CEM II); (ii) 50% CEM II /50% CKD (PresafeP); (iii) 50% CEMII/ 50% LKD (Spectra); and (iv) 50% CEMII/30% LKD (Spectra) /20% LS filler. Water demand was the highest for binder of combinations 50% CEM II and 50% CKD and for 50% CEM II, 30% LKD, and 20% limestone filler. Water requirement for 50% CEM II and 50% LKD was the same as for pure CEM II. The bonding time varied from 165 to 250 min. The admixtures with 50% LKD and 50% CKD had a significantly longer setting time compared to the CEM II (Figure 9). Four tested combinations of binders include the following mixtures (from left to right in Figure 9): (i) 100% cement (CEM II); (ii) 50% CEM II /50% CKD (PresafeP); (iii) 50% CEM II/50% LKD (Spectra); and (iv) 50% CEM II / 30% Spectra(LKD)/20% LSfiller.

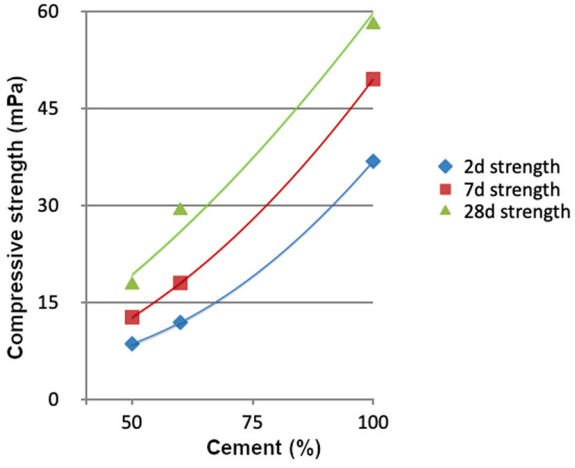

Figure 8: Compressive strength as a function of cement content for varied curing time.

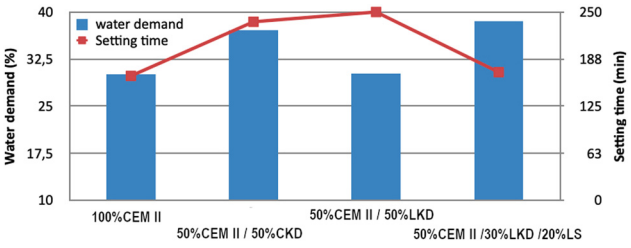

Figure 9: Water requirement and setting time for different combinations of binders: Cement (CEM-II), CKD, LKD and LS.

Figure 10 shows a comparison of the compressive strength of the specimens stabilised with different recipes without adding clay admixture. Recipe A (100% cement) shows the highest values (up to 20 MPa by sample 8) and always outperforms all the other recipes in terms of strength, which means that cement remains the most effective stabiliser for clay. Following that, Recipe B (70% cement, 30% LKD) also shows high values with maximum achieved at sample 7 (13.8 MPa). Recipe C has been less effective with added 80% cement and 20% CKD. Such binder combination has shown the highest value of UCS as 8.8 MPa in sample 9. Finally, the least strength was demonstrated in Recipe D (70% cement, 30% CKD) where the UCS values never exceeded 4 MPa with maximal values of 3.7 at sample 2 and the lowest UCS as 2.7 MPa at sample 3 (Figure 10).

Figure 11 shows a nonlinear dependence of the P-wave velocity as a function of curing time for Recipes A to D. Each P-wave velocity determination is an average of measurements on five specimens with binder recipes corresponding to the following equations: Recipe A – Eq. (3); Recipe B – Eq. (4); Recipe C – Eq. (5); Recipe D – Eq. (6).

$$y = 136.79\ln(x) + 1913.5;\ R^2 = 0.9979, \quad (3)$$

$$y = 190.38\ln(x) + 1{,}620;\ R^2 = 0.9994, \quad (4)$$

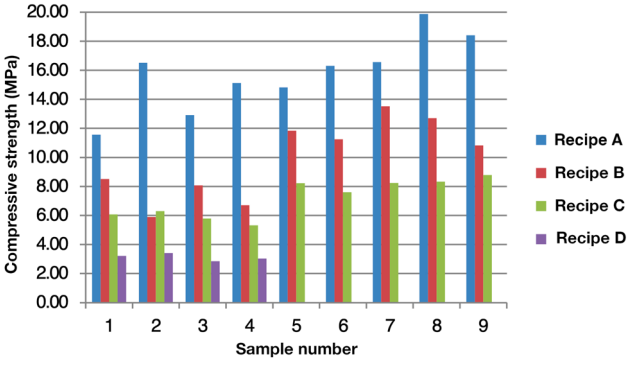

Figure 10: Compilation of the compressive strength of the various binder combinations without mixing clay.

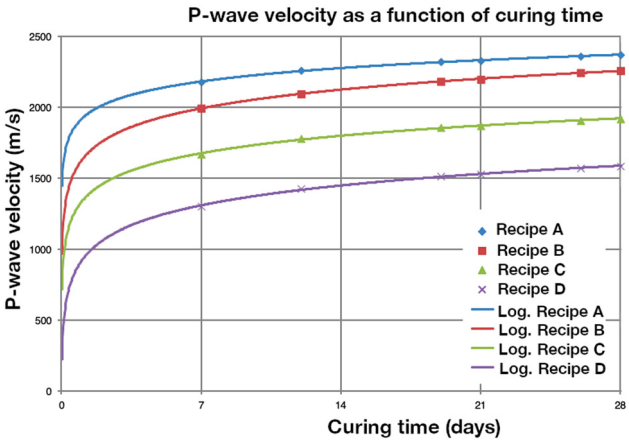

Figure 11: *P*-wave velocity over curing time at 20 °C.

$$y = 177.54\ln(x) + 1328.5;\ R^2 = 0.9968, \quad (5)$$

$$y = 201.68\ln(x) + 913.98;\ R^2 = 0.9970. \quad (6)$$

Here, Recipe A (100% cement) shows the most effective results outperforming the other blended mixtures with the P-wave velocity at 2,350 m/s on day 28.

Figure 12 shows a compilation of the measured P-wave velocities and compressive strength for different binder recipes. Considering the empirical distribution of the data points on the regression line, Figure 12 depicts that Recipe D (70% cement 30% CKD) has the lowest P-wave velocity (1,600 m/s), which corresponds to the 4.0–4.4 MPa of UCS. In the next example, Recipe C (80% cement, 20% CKD) shows that P-wave velocity varies from 1,900 to 1,950 m/s with UCS at 7.5–9 MPa. Following that, the specimens stabilised with Recipe B (70% cement, 30% LKD) achieved much higher UCS

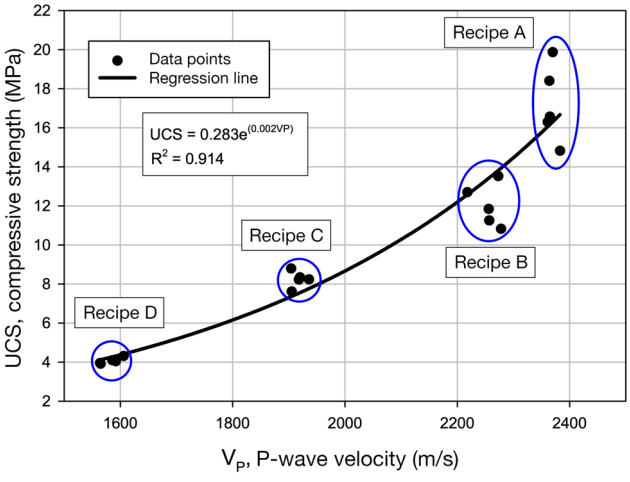

Figure 12: Compressive strength as a function of P-wave velocity for recipes A to D. Samples stored for 28 days at 20 °C.

between 10.7 and 13.8 MPa, which corresponds to the P-wave velocity at 2,210–2,300 m/s. Finally, a quick visual inspection shows that Recipe A (100% cement) has the best performance in terms of clay stabilisation with tested samples having UCS from 14.4 to 20.0 MPa and a corresponding P-wave velocity varying between 2,350 and 2,400 m/s (Figure 12).

Figure 13 shows the compressive strength of samples stabilised with various binder recipes with different admixtures of clay during 28 days at 20 °C. For binder Recipe A, the UCS between 11.5 and 19.8 MPa was obtained for specimens consisting of binder and water (Figure 13). When clay was added into a mixture, strength dropped to a minimum of 4 MPa for a mixture of 58% clay (Figure 13). For the binder Recipe B without mixing clay, the compressive strength values were recorded in a range between 5.9 and 13.3 MPa.

In clay mixture of 58%, the compressive strength dropped to approximately 3.2 MPa at its lowest value. For the binder Recipe C, the compressive strength between 5.3 and 8.8 MPa was obtained without adding clay into the mixture. At the same time, when adding clay into the mixture up to 58%, the compressive strength dropped to 3.6 MPa. For binder Recipe D without clay mixing, the values of compressive strength were 2.8 and 4.3 MPa (Figure 13).

The specimen stabilised by Recipe B (70% cement, 30% LKD) demonstrated P-wave velocity as 2,350 m/s achieved on the same day. Recipe C (80% cement, 20% CKD) and Recipe D (70% cement 30% CKD) demonstrated P-wave velocity 1,900 and 1,550 m/s, respectively. All the specimens demonstrated a gain of the UCS, which corresponds to the sharp increase of the P-wave speed during the first 3 days of curing. Afterwards, the behaviour of strength gain stabilised, as shown in the graphs demonstrating a logarithmic growth in curve of the correlation between the P-wave speed and curing time. The comparison of the performance of binder blends shows that Recipe B (70% cement, 30% LKD) has better results for the P-wave velocity as a function of curing time, compared to other mixtures (Figure 11).

Figure 14 shows heat development with the two different binder combinations as a function of time. The results show significantly lower values for binders with 50% CEM II and 50% LKD, compared to 100% CEM II. However, both mixtures show a similar time course from mixing until the maximum temperature is obtained. The double experiments demonstrated a good repeatability with approved results in the repeated experiments with soil samples. The results of the performed temperature development for binder slurry are shown in Figure 14.

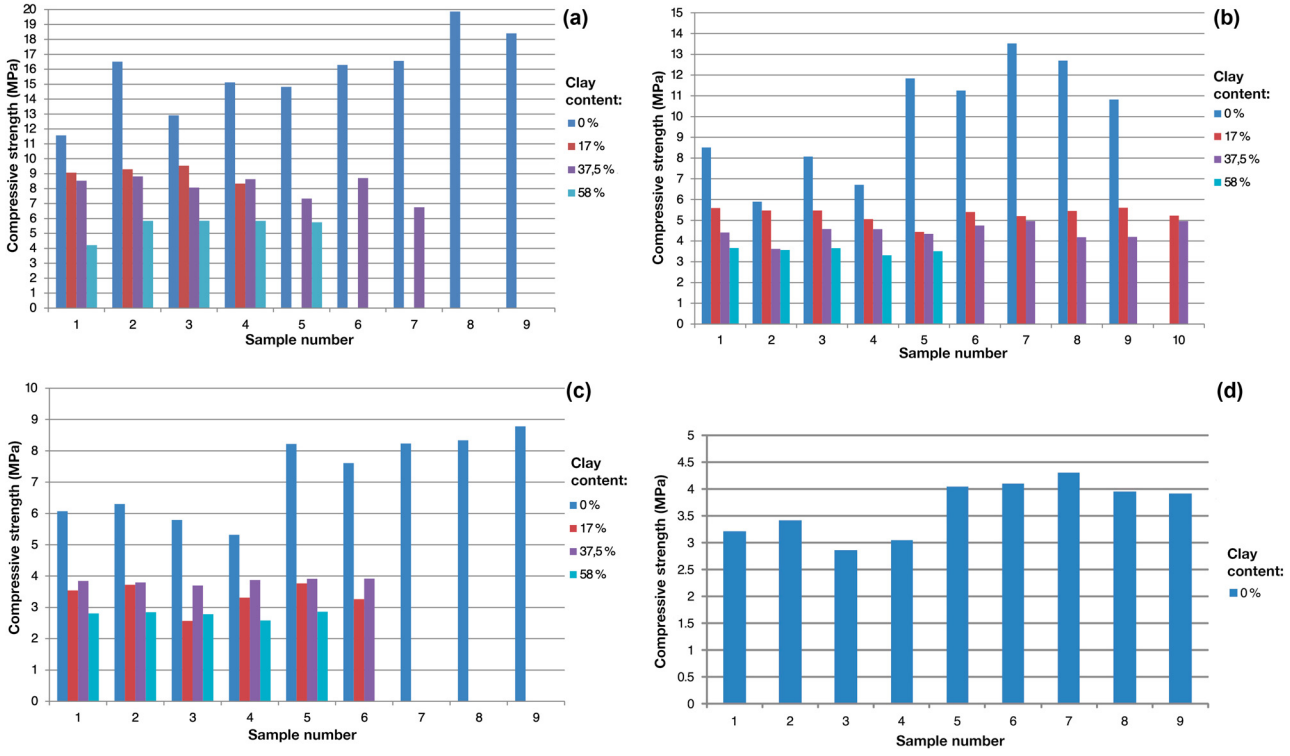

Figure 13: Compressive strength of sample stabilised with various binder recipes with different admixtures of clay during 28 days at 20 °C. (a) CEM II/A-M; (b) 70% CEM II/A-M and 30% LKD; (c) 80% CEM II/A-M and 20% CKD; (d) 70% CEM II/A-M and 30% CKD.

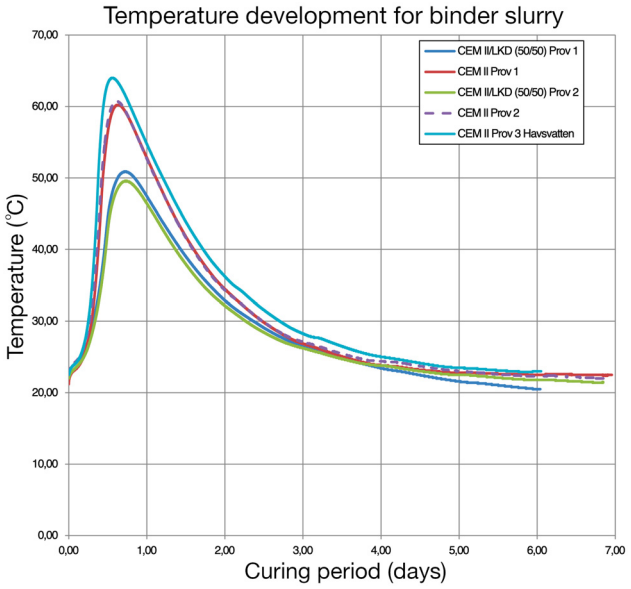

Figure 14: Heat development in two binder combinations over time.

Several mixtures that contained all the binders, *i.e.*, cement, quicklime, CKD, and LKD, met the requirements of at least 200 kPa after 28 days of storage. At a storage temperature of 7 °C, final strength is reached at 80 days at the earliest, which demonstrated excellent performance. For jet grouting, the *in situ* requirement is that a compressive strength has 2 MPa after 28 days of curing. For samples processed in the laboratory, the requirement is set to at least 3 MPa after 28 days of curing. The graphs demonstrated that binders with Recipes A and B passed this requirement even with a mixture of 58% clay. For binder of Recipe C, the mean UCS was 2.77 MPa with a clay mix of 58%. As a result of the performed works, soil specimens increased in strength: the UCS (compressive strength) and bond shear strength, as well as the related parameters, such as lower permeability and reduced compressibility.

3.3 Simulation of seismic measurements

Geophysical methods for evaluating soil strength by measuring P-wave velocity present a nondestructive advanced approach, which enables us to mitigate the costs of construction works and to replace the time-consuming and technically difficult workflow of measuring soil strength in real-time conditions. The applied geophysical method of measuring P-wave velocities is particularly efficient in terms of production costs. In fact, the price of soil stabilisation scales progressively with the increased amount of binders. This is because the workload and the methodology of testing strength of foundations is a highly time consuming and laborious work in construction industry and geotechnical works.

With this regard, the application of the geophysical methods reduces the expenses in the industrial projects and enables to test soil strength using nondestructive methods. In addition, despite the best performance of cement as a pure binder, variations with other admixtures may help in reducing negative environmental effects from cement and assisting with utilisation of the industrial by-products using as auxiliary binders.

The simulated models of the natural frequency obtained from seismic measurements performed in the laboratory aims at natural frequency analysis. It is used to determine the dynamic inherent properties of a soil system without sleeves and to identify its resonant frequencies as eigen values. Thus, it visualises a frequency at which the amplitude of the vibration is the highest when exited by the external means, that is, using simulation software. A sleeve without soil had natural frequencies in the same order of magnitude as the sample itself, which is shown on the biased plots (Figure 15).

Figure 15 shows the inverse task, which shows simulation of different modes of natural frequency for empty pipe sleeves without soil. It is modelled for the three cases: 1,707, 1,767, and 3,870 Hz. The first case represents the uniform pattern of colours with the modelled pipe corresponding to the height and diameter of the real pipe and its natural frequencies. In the second case, the frequencies are higher in the upper and lower parts of the pipe. The third case has an irregular form of the pipe column (Figure 15).

Figure 16 shows simulated natural frequencies for the specimens without a sleeve using modelled form. By simulating the test bodies placed in sleeves, natural frequencies are used as modelled data. The model can generally be described as simulated natural frequencies for the specimens without sleeve for the test bodies, which have a length of 130.7 mm and varied frequencies, so that the phenomenon of the fundamental lowest frequency exhibits its effects at different values of frequency: 1,070, 2,014, 2,208, and 3,393 Hz (Figure 16).

Figure 17 shows the simulation plots that measured natural frequencies that originated from the parts of the sleeves containing soil material. This is performed to estimate own frequencies of the pipes and to correct possible bias in evaluating the P-wave velocities, while testing stabilised soil. The aim is to predict and avoid the resonance with the excitation vibration in soil samples. Using simulation software, the values were visualised as 3D plots making it straightforward to interpret (Figure 17).

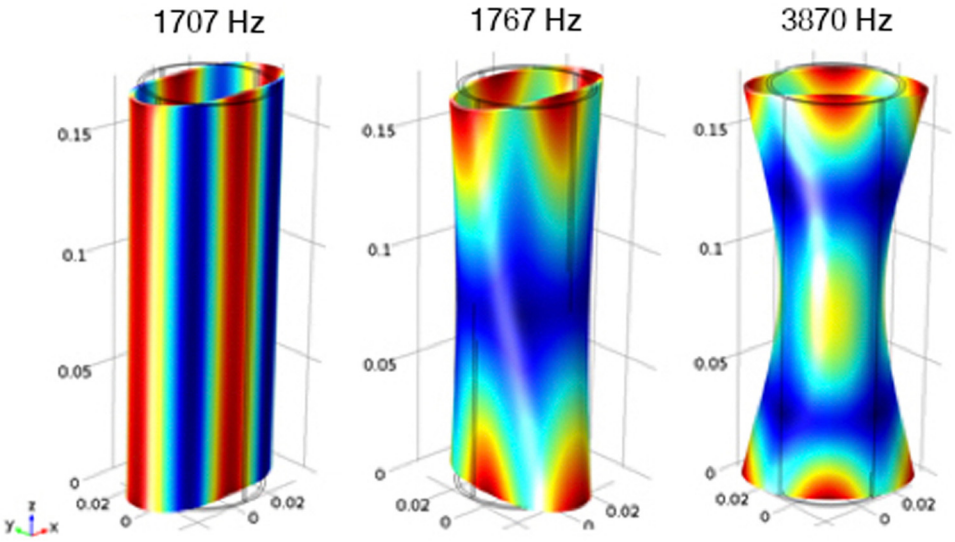

Figure 15: Simulations of the natural frequency for pipe sleeves.

4 Discussion

Subject to the diameter of the grouting columns and percentage of lime/cement stabilisers, a hundred thousand of tons of cement are required for deep stabilisation per year for construction industry in Sweden. This necessarily involves significant financial investments for the production of binder materials. To reduce this cost, industrial by-products, such as LKD and Ql are used to replace a part of pure cement. Such a replacement not only enables to economise the costs of earthworks in construction industry but also has sound technical and environmental benefits.

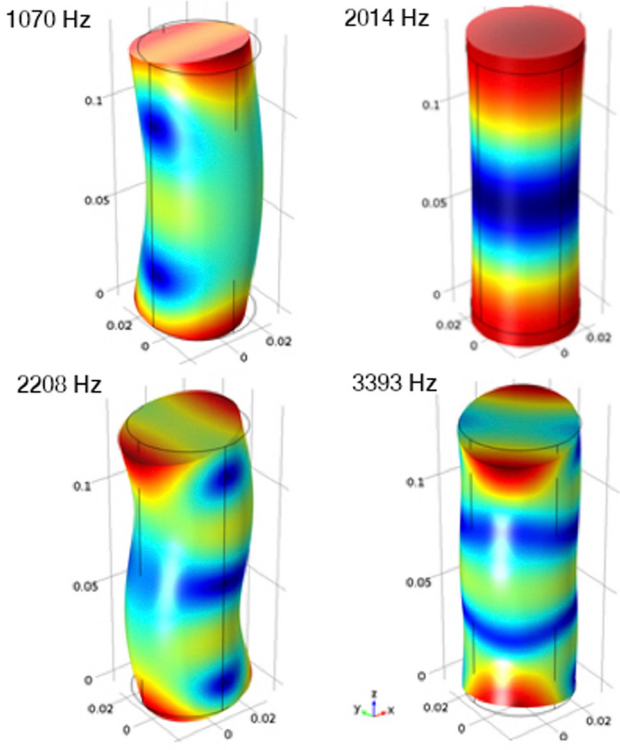

Figure 16: Calculated natural frequencies for specimens without sleeve. The test bodies have a length of 130.7 mm.

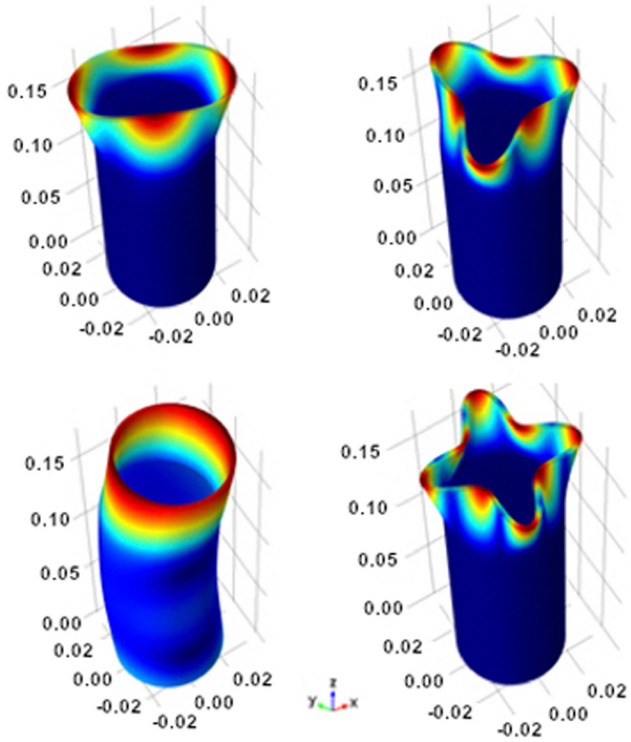

Figure 17: Simulated natural frequencies for sample in sleeve. Sample body 130.7 and sleeve 170 mm.

In this article, we demonstrated that a combination of LKD, Ql, CKD, and OPC instead of pure OPC has positive effects on deep soil stabilisation by jet grouting. The laboratory testing showed a high repeatability between the trials with various binder combinations.

The variations in compressive strength and shear strength increased slightly along with curing time, which is expected, since minor inaccuracies in the test specimens have a greater effect. For comparison with various binder amounts, the analysis was performed with the same number of tests for 80, 100, and 120 kg of binder. The requirements for the lime/cement columns *in situ* are achieved during the tests: a minimum shear strength of 150 kPa after 28 days of curing. This is ensured by the requirement for laboratory packed samples, which is set to >200 kPa. The P-wave velocity is an index for the changes in strength. It has been measured using the ceramic shear ICP® accelerometer and vibration induced by a hammer and presented on graphs showing correlation between the P-wave velocity and the UCS.

The construction industry is strongly dependent on the advanced technologies of soil improvement. The most challenging issue in construction techniques consists in finding the optimal solutions for the best results in soil stabilisation. While the recommendations regarding ground improvement and reviews of general standards of soil testing are available in the existing technical engineering documentation, more complex issues related to the nonlinear analysis of soil behaviour and strength properties tested by geophysical methods require special studies.

The stability of foundations in building construction strongly depends on soil strength. In process of stabilisation, the strength of soil increases over time of curing. This improves the present conditions of the ground and mitigates future risks of the instability of buildings and roads constructed on a weak ground. The performance of stabilisation should always be evaluated and assessed according to the existing standards and threshold values of UCS, accepted by the existing norms of civil engineering.

In response to the needs of developing effective methods of testing soil strength to evaluate the effects of various binders on soil stabilisation, an optimised design of experiments on soil improvement and the quality control for strength in soil are presented in this article. The workflow included advanced statistical methods of data processing to monitor and evaluate the effects from various combinations of binders on soil stabilisation. Several simplex experiments were performed on soil–binder mixing, equivalent to 80, 100, and 120 kg of binder per m^3 of clay.

5 Conclusion

This study presented an application of geophysical testing of compression wave velocity (P-wave) and measuring shear bond and compressive strength (UCS) of soil specimens. A special focus of this article is placed on presenting the four different binders and evaluating the behaviour of soil using various amounts and ratio of binders used as stabilising agents: CEM II/A contained of Portland clinker and limestone), burnt lime, CKD, and LKD. The CKD was applied for extra tests in jet grouting.

Specifically, the main contributions of this article are summarised as the following issues:

1) We proposed to combine four different binders for soil stabilisation (i) CEM II/A, a Portland limestone cement; (ii) burnt lime; (iii) LKD up to 50%; (iv) CKD and evaluated the gain in soil strength over curing period for samples stabilised by combinations of these binders mixed in various proportions.
2) We introduced a simple yet efficient robust algorithm of testing optimal combinations of binders using statistical simplex centroid design. Since the amounts of soil tested in real projects may exceed several tons, finding the best solutions for binder combinations through modelling significantly reduces the price of work and increases the optimisation of the workflow on soil stabilisation.
3) We demonstrated that the application of the statistical methods of combinatorics applied for engineering projects effectively describes the behaviour of soil hardened by stabilising agents. Here, an optimal solution of selection of binders is achieved by iteratively checking soil strength criteria. The process was repeated until the models shown stable solutions for proportions of binders.
4) We developed an approach of seismic measurements for evaluation of soil strength using nondestructive methods by evaluating the velocity of P waves, which directly correspond to the strength of soil as a complex porous media consisting of solid particles and groundwater which determines its elasticity, compressibility, and compactness.
5) We carried out extensive experiments on soil measurements supported by graphs showing the dynamics of shear strength in specimens stabilised by various binders, and response surface plots showing showing shear strength after 28 days of curing, that is, late strength development in soil with changed amount of binders – 80, 100, and 120 kg/m^3.
6) We evaluated the compressive strength of specimens with different ratios of binders: cement (CEM II), CKD,

LKD, and LS. We show that shear strength can be represented as an exponential curve of P-wave velocity. Moreover, we assessed the compressive strength as a function of cement over curing period on 2nd, 7th, and 28th day of curing.

Acknowledgement: We thank Prof. Dr. Nils Rydén from Lund University for his help with the simulation modelling using COMSOL Multiphysics software. We appreciate the valuable comments of the two anonymous reviewers which improved the initial version of this manuscript.

Funding information: The authors state no funding involved.

Author contributions: Both authors wrote text of the manuscript, performed data analysis, literature review, discussion, and interpretation of the results. Dr. Per Lindh supervised the project. Both authors are responsible for the content of this manuscript, read and accepted the paper, and approved its submission.

Conflict of interest: The authors declare that the research was conducted in the absence of any commercial or financial relationships that could be construed as a potential conflict of interest.

References

[1] Jenny H. Factors of soil formation: a system of quantitative pedology. Garden City (NY), USA: Dover Earth Science; 2011.
[2] Buol SW, Southard RJ, Graham RC, McDaniel PA. Soil genesis and classification. 6th ed. Malden (MA), USA: Wiley-Blackwell; 2011.
[3] Winterkorn HF, Fang HY. Soil technology and engineering properties of soils. Boston (MA), USA: Springer US; 1991. p. 88–143.
[4] Righi D, Meunier A. Origin of clays by rock weathering and soil formation. Berlin, Heidelberg: Springer Berlin Heidelberg; 1995. p. 43–161.
[5] Nesse WD. Introduction to mineralogy. 2nd ed. Oxford, UK: Oxford University Press; 2012.
[6] Källán H, Heyden A, Lindh P. Estimation of grain size in asphalt samples using digital image analysis. In: Tescher AG, editor. Applications of digital image processing XXXVII. Vol. 9217. Bellingham (WA), USA: International Society for Optics and Photonics. SPIE; 2014. p. 292–300.
[7] Källán H, Heyden A, Åström K, Lindh P. Measuring and evaluating bitumen coverage of stones using two different digital image analysis methods. Measurement. 2016;84:56–67.
[8] Golewski GL. On the special construction and materials conditions reducing the negative impact of vibrations on concrete structures. In: Serban VA, Marsavina L, Utu D, Linul E, editors. Materials Today: Proceedings. 8th International Conference on Advanced Materials and Structures – AMS 2020. Amsterdam: Elsevier Ltd. 2020. Vol. 458; 2021. p. 4344–8.
[9] Nascimbene R, Bianco L. Cyclic response of column to foundation connections of reinforced concrete precast structures: numerical and experimental comparisons. Eng Struct. 2021;247:113214.
[10] Golewski GL. The specificity of shaping and execution of monolithic pocket foundations (PF) in hall buildings. Buildings. 2022;12(2):192.
[11] Zhang P, Han S, Golewski GL, Wang X. Nanoparticle-reinforced building materials with applications in civil engineering. Adv Mech Eng. 2020;12(10):1687814020965438.
[12] Lindh P, Lemenkova P. Permeability, compressive strength and Proctor parameters of silts stabilised by Portland cement and ground granulated blast furnace slag (GGBFS). Archive Mech Eng. 2022;69:1–26.
[13] Gil DM, Golewski GL. Potential of siliceous fly ash and silica fume as a substitute for binder in cementitious concretes. In: Lichołai, Dęska B, Miąsik P, Szyszka J, Krasoń J, Szalacha A, editors. SOLINA 2018 - VII Conference SOLINA Sustainable Development: Architecture - Building Construction - Environmental Engineering and Protection Innovative Energy-Efficient Technologies - Utilization of Renewable Energy Sources; 2018 Jun 19–13; Polańczyk, Poland. EDP Sciences, 2018. Article Nr. 00030.
[14] Golewski GL, Bartosz S. Strength and microstructure of composites with cement matrixes modified by fly ash and active seeds of C-S-H phase. Struct Eng Mech. 2022;82(4):543–56.
[15] Modoni G, Croce P, Mongioviiii L. Theoretical modelling of jet grouting. Géotechnique. 2006;56(5):335–47.
[16] Croce P, Flora A, Modoni G. Jet grouting: technology, design and control. Boca Raton (FL), USA: CRC Press; 2014.
[17] Modoni G, Wanik L, Mascolo Maria C, Salvatore E, Bzóka J, Shui-Long S, et al. Strength of sandy and clayey soils cemented with single and double fluid jet grouting. Soils Found. 2019;59(4):942–54.
[18] Mosiici P. Jet grouting quality control. Institution Civil Engineers; 1994. p. 227–35.
[19] Covil CS, Skinner AE. Jet grouting – a review of some of the operating parameters that form the basis of the jet grouting process. Westminster, London, UK: Institution of Civil Engineers; 1994. p. 605–29.
[20] Njock PGA, Chen J, Modoni G, Arulrajah A, Kim YH. A review of jet grouting practice and development. Arabian J Geosci. 2018;11(16):1–31.
[21] Morey J, Campo DW. Quality control of jet grouting on the Cairo metro. Proc Instit Civil Eng Ground Improvement. 1999;3(2):67–75.
[22] Yoshida H. Recent developments in jet grouting. Reston (VA), USA: American Society of Civil Engineers; 2012. p. 1548–61.
[23] Lunardi P. Ground improvement by means of jet-grouting. Proc Inst Civ Eng: Ground Improv. 1997;1(2):65–85.
[24] Modoni G, Bzoooowka J. Analysis of foundations reinforced with jet grouting. J Geotech Geoenviron Eng. 2012;138(12):1442–54.

[25] Modoni G, Bzówka J. Analysis of foundations reinforced with jet grouting. J Geotech Geoenviron Eng. 2012;138(12):1442–54.
[26] Pinto A, Tomáio R, Pita X, Pereira A. Ground treatment solutions using jet grouting. Reston (VA), USA: American Society of Civil Engineers; 2012. p. 2112–21.
[27] Croce P, Modoni G, Russo G. Jet-grouting performance in tunnelling. Reston (VA), USA: American Society of Civil Engineers; 2004. p. 910–22.
[28] Hamidi B, Yates M, Berthier D, Krzeminski M. Overcoming challenges with jet grouting at sydney international airport. Reston (VA), USA: American Society of Civil Engineers; 2012. p. 2092–101.
[29] Lewis DA, Taube MG. North airfield drainage improvement at Chicago-OaHare international airport: soil stabilisation using jet grouting. Reston (VA), USA: American Society of Civil Engineers; 2003. p. 464–73.
[30] Farr SJ, Camper KE, Byford BM. Jet grouting for earth retention performed in low headroom for subway station expansion. Reston (VA), USA: American Society of Civil Engineers; 2012. p. 963–71.
[31] Chu HC, Wong KN, Yu CF, Liao HJ, Cheng SH. Large diameter rapid jet grouting in taipei silty soil. Reston (VA), USA: American Society of Civil Engineers; 2012. p. 2132–41.
[32] Mihalis IK, Tsiambaos G, Anagnostopoulos A. Jet grouting applications in soft rocks: the Athens Metro case. Proc Institution Civil Engineers Geotech Eng. 2004;157(4):219–28.
[33] Newman RL, Essler RD, Covil CS. Jet grouting to enable basement construction in difficult ground conditions. Westminster, London, UK: Institution of Civil Engineers; 2015. p. 385–402.
[34] Chu HC, Wong KN, Yu CF, Liao HJ, Cheng SH. Large diameter rapid jet grouting in Taipei silty soil. Reston (VA), USA: American Society of Civil Engineers; 2012. p. 2132–41.
[35] Ho CE, Hu S. Jet grouting for the mitigation of excavation wall movements in glacial silts. Reston (VA), USA: American Society of Civil Engineers; 2014. p. 128–37.
[36] Ho CE, Lim CH, Tan CG. Jet grouting applications for large-scale basement construction in soft clay. Reston (VA), USA: American Society of Civil Engineers; 2005. p. 1–15.
[37] Ho CE. Analysis of deep jet grouting field trial in clay. Reston (VA), USA: American Society of Civil Engineers; 2009. p. 233–40.
[38] Han WJ, Liu SY, Zhang DW, Du G. Field behavior of jet grouting pile under vacuum preloading of soft soils with deep sand layer. Reston (VA), USA: American Society of Civil Engineers; 2012. p. 70–7.
[39] Kitazume M, Terashi M. The deep mixing method. Vol. 21. London: CRC Press; 2013.
[40] Porbaha A. State of the art in deep mixing technology: Part I. Basic concepts and overview. Proc Inst Civ Eng: Ground Improv. 1998;2(2):81–92.
[41] Larsson S, Stille H, Olsson L. On horizontal variability in lime-cement columns in deep mixing. London, UK: Thomas Telford Limited; 2015. p. 21–32.
[42] Larsson S, Dahlström M, Nilsson B. A complementary field study on the uniformity of lime-cement columns for deep mixing. Proc Inst Civ Eng: Ground Improv. 2005;9(2):67–77.
[43] Porbaha A, Tanaka H, Kobayashi M. State of the art in deep mixing technology: part II. Applications. Proc Inst Civ Eng: Ground Improv. 1988;2(3):125–39.
[44] Dahlström M, Wiberg D. Dry soil mixing and vibro replacement in combination for a high embankment. Reston (VA), USA: American Society of Civil Engineers; 2012. p. 565–74.
[45] Xie SH, Liu SY, Liu ZB, Du GY. In situ test on soft marine clays with high clay content improved by bidirectional dry jet mixing method. Reston (VA), USA: American Society of Civil Engineers; 2012. p. 988–95.
[46] Porbaha A, Shibuya S, Kishida T. State of the art in deep mixing technology. Part III: geomaterial characterization. Proc Inst Civ Eng: Ground Improv. 2000;4(3):91–110.
[47] Fang YS, Chung YT, Yu FJ, Chen TJ. Properties of soil-cement stabilised with deep mixing method. Proc Inst Civ Eng: Ground Improv. 2001;5(2):69–74.
[48] Mypati VNK, Saride S. Feasibility of alkali-activated low-calcium fly ash as a binder for deep soil mixing. J Mater Civil Eng. 2022;34(1):04021410.
[49] Bergado DT, Ruenkrairergsa T, Taesiri Y, Balasubramaniam AS. Deep soil mixing used to reduce embankment settlement. Proc Inst Civ Eng: Ground Improv. 1999;3(4):145–62.
[50] Munfakh GA. Ground improvement engineering – the state of the US practice: part 1. Methods. Proc Inst Civ Eng: Ground Improv. 1997;1(4):193–14.
[51] Winterkorn HF, Pamukcu S. Soil stabilisation and grouting. Boston, MA: Springer US; 1991. p. 317–78.
[52] Robertson JB, Ley MT, Cook MD. Measuring the change in water-to-cement ratio in fresh and hardened concrete. J Mater Civil Eng. 2022;34(4):04022016.
[53] Zhang Q, Liu J, Liu J, Han F, Lin W. Effect of superplasticizers on apparent viscosity of cement-based material with a low water-binder ratio. J Mater Civil Eng. 2016;28(9):04016085.
[54] Yang KH, Hwang HZ, Lee S. Effects of water-binder ratio and fine aggregate-total aggregate ratio on the properties of Hwangtoh-based alkali-activated concrete. J Mater Civil Eng. 2010;22(9):887–96.
[55] Rabbi ATMZ, Kuwano J. Effect of curing time and confining pressure on the mechanical properties of cement-treated sand. Reston (VA), USA: American Society of Civil Engineers; 2012. p. 996–1005.
[56] Xu J, Xu C, Yoshimoto N, Hyodo M, Kajiyama S, Huang L. Compression and deformation characteristics of hydrate-bearing sediments under high effective confining pressure. Int J Geomech. 2022;22(6):04022067.
[57] Huang J, Chen J, Yu S, Fu X, Zhang G, Tian N. Dynamic behaviors of overconsolidated clay under cyclic confining pressure. Int J Geomech. 2022;22(11):04022197.
[58] Jiang H, Zhang J, Jiang R. Stress evaluation for rocks and structural concrete members through ultrasonic wave analysis: review. J Mater Civil Eng. 2017;29:04017172.
[59] Jiang H, Zhan H, Zhang J, Jiang R, Zhuang C, Fan P. Detecting stress changes and damage in full-size concrete T-beam and slab with ultrasonic coda waves. J Struct Eng. 2021;147:04021140.
[60] Lacidogna G, Piana G, Carpinteri A. Damage monitoring of three-point bending concrete specimens by acoustic emission and resonant frequency analysis. Eng Frac Mech. 2019;210:203–11.
[61] Lin S, Wang Y. Crack-depth estimation in concrete elements using ultrasonic shear-horizontal waves. J Perform Constr Facil. 2020;34:04020064.

[62] Askeland DR, Fulay PP. Essentials of Materials Science & Engineering. Mason (OH), USA: Cengage Learning; 2008. https://books.google.be/books?id=LxJtCgAAQBAJ.
[63] Askeland D, Fulay P. The Science & Engineering of Materials. Mason (OH), USA: Cengage Learning; 2005. https://books.google.be/books?id=fRbZslUtpBYC.
[64] Sarno A, Farah R, Hudyma N, Hiltunen DR. Relationships between compression wave velocity and unconfined compression strength for weathered florida limestone. Reston (VA), USA: American Society of Civil Engineers; 2010. p. 950–9.
[65] Pellet FL, Fabre G. Damage evaluation with P-wave velocity measurements during uniaxial compression tests on argillaceous rocks. Int J Geomech. 2007;7(6):431–6.
[66] Gheibi A, Hedayat A. Ultrasonic investigation of granular materials subjected to compression and crushing. Ultrasonics. 2018;87:112–25.
[67] Sarro WS, Assis GM, Ferreira GCS. Experimental investigation of the UPV wavelength in compacted soil. Constr Build Mater. 2021;272:121834.
[68] Shi Z, Wen Y, Meng Q. Propagation attenuation of plane waves in saturated soil by pile barriers. Int J Geomech. 2017;17:04017053.
[69] Carpinteri A, Lacidogna G, Pugno N. Structural damage diagnosis and life-time assessment by acoustic emission monitoring. Eng Fract Mech. 2007;74:273–89.
[70] Aggelis DG. Classification of cracking mode in concrete by acoustic emission parameters. Mech Res Commun. 2011;38:153–7.
[71] DiSante M, Fratalocchi E, Mazzieri F, Pasqualini E. Prediction of shear strength parameters in soil-lime mixture design – part 1: quicklime. Proc Inst Civ Eng: Ground Improv. 2020;173(2):93–104.
[72] Lindh P, Lemenkova P. Impact of strength-enhancing admixtures on stabilisation of expansive soil by addition of alternative binders. Civil Environ Eng. 2022;18(2):726–35. doi: 10.2478/cee-2022-0067.
[73] Lindh P, Lemenkova P. Soil contamination from heavy metals and persistent organic pollutants (PAH, PCB and HCB) in the coastal area of Västernorrland, Sweden. Gospodarka Surowcami Mineralnymi Mineral Resources Management. 2022;38:147–68.
[74] Brice M, Smith N, Pallett PF, Filip R. Lime and cement stabilisation. London, England, UK: ICE Publishing; 2019. p. 91–9.
[75] Heath DC. The application of lime and cement soil stabilisation at BAA airports. Proc Inst Civ Eng: Ground Improv. 1992;95(1):11–50.
[76] Addison MB, Polma FA. Extending durability of lime modified clay subgrades with cement stabilisation. Reston (VA), USA: American Society of Civil Engineers; 2007. p. 1–10.
[77] Rogers CD, Boardman DI, Papadimitriou G. Stress path testing of realistically cured lime and lime/cement stabilised clay. J Mater Civil Eng. 2006;18(2):259–66.
[78] Solanki P, Khoury N, Zaman MM. Engineering properties and moisture susceptibility of silty clay stabilised with lime, class C fly ash, and cement Kiln dust. J Mater Civil Eng. 2009;21(12):749–57.
[79] Mitchell JK, Greenberg JA, Witherspoon PA. Chemico-osmotic effects in fine-grained soils. J Soil Mech Found Div. 1973;99(4):307–22.
[80] Wang HG, Xu LR, Chen JJ, Lv DW. Study on the strength mechanism of coarse-grained soil influenced by clay content based on laboratory test. Reston (VA), USA: American Society of Civil Engineers; 2009. p. 14–9.
[81] Lambe TW. Physico-chemical properties of soils: role of soil technology. J Soil Mech Found Div. 1959;85(2):55–70.
[82] Lindh P. Optimizing binder blends for shallow stabilisation of fine-grained soils. Proc Inst Civ Eng: Ground Improv. 2001;5:23–34.
[83] Guo T, Geaghan JP, Rusch KA. Determination of optimum ingredients for phosphogypsum composite stability under marine conditions-response surface analysis with process variables. J Environ Eng. 2003;129(4):358–65.
[84] Lindh P. Compaction- and strength properties of stabilised and unstabilised fine-grained tills. Lund, Sweden: Lund University; 2004.
[85] Glendinning S, Rogers CDF. Deep stabilisation using lime. London: Telford Services Limited; 1996. p. 127–38.
[86] Lindh P, Lemenkova P. Geochemical tests to study the effects of cement ratio on potassium and TBT leaching and the pH of the marine sediments from the Kattegat Strait, port of Gothenburg, Sweden. Baltica. 2022;35:47–59.
[87] Nigitha D, Prabhanjan N. Efficiency of cement and lime in stabilising the black cotton soil. Mater Today: Proc. 2022;68(5):1588–93.
[88] Lemenkov V, Lemenkova P. Using tex markup language for 3D and 2D geological plotting. Found Comput Decis Sci. 2021;46:43–69.
[89] Hov S, Paniagua P, Sæetre C, Rueslåtten H, Størdal I, Mengede M, et al. Lime-cement stabilisation of Trondheim clays and its impact on carbon dioxide emissions. Soils Found. 2022;62(3):101162.
[90] Bakaiyang L, Madjadoumbaye J, Boussafir Y, Szymkiewicz F, Duc M. Re-use in road construction of a Karal-type clay-rich soil from North Cameroon after a lime/cement mixed treatment using two different limes. Case Stud Constr Mater. 2021;15:e00626.
[91] Golewski GL. Physical characteristics of concrete, essential in design of fracture-resistant, dynamically loaded reinforced concrete structures. Mater Desi Process Commun. 2019;1(5):e82. E82 MDPC-2019-028.R1.
[92] Lindh P, Winter MG. Sample preparation effects on the compaction properties of Swedish fine-grained tills. Q J Eng Geol Hydrogeol. 2003;36:321–30.
[93] Lemenkov V, Lemenkova P. Testing deformation and compressive strength of the frozen fine-grained soils with changed porosity and density. J Appl Eng Sci. 2021;11:113–20.
[94] Lemenkov V, Lemenkova P. Measuring equivalent cohesion ceq of the frozen soils by compression strength using kriolab equipment. Civil Environ Eng Rep. 2021;31:63–84.
[95] Sato A, Yamanashi T, Suzuki T, Kawabata S. Land-improvement technology using the heat of soil stabiliser reactions in cold regions. Reston (VA), USA: ASCE; 2015. p. 170–80.
[96] Montgomery DC. Design and analysis of experiment. 10th ed. New Jersey, US: Wiley; 2019.
[97] Myres RH, Montgomery DC, Anderson-Cook CM. Response surface methodology: process and product optimization using designed experiments. 4th ed. New Jersey, US: Wiley; 2016.
[98] Lindh P, Lemenkova P. Evaluation of different binder combinations of cement, slag and CKD for S/S treatment of TBT

contaminated sediments. Acta Mech et Autom. 2021;15:236–48.
[99] Lindh P, Lemenkova P. Simplex lattice design and X-ray diffraction for analysis of soil structure: a case of cement-stabilised compacted tills reinforced with steel slag and slaked lime. Electronics. 2022;11(22).
[100] Carlsten P. Chapter 10. Lime and lime/cement columns. In: Hartlén J, Wolski W, editors. Developments in Geotechnical Engineering. Amsterdam, The Netherlands: Elsevier; 1996. p. 355–99.
[101] Lindh P, Lemenkova P. Seismic velocity of P-waves to evaluate strength of stabilised soil for Svenska Cellulosa Aktiebolaget Biorefinery AAA-strand AB, Timrå. B Poli Acad Sci Tech Sci. 2022;70:1–9.
[102] Lindh P, Lemenkova P. Resonant frequency ultrasonic P-waves for evaluating uniaxial compressive strength of the stabilised slag cement sediments. Nordic Concr Res. 2021;65:39–62.
[103] Ryden N, Ekdahl U, Lindh P. Quality control of cement stabilised soil using non-destructive seismic tests. DGZfp - Proceedings Advanced Testing of Fresh Cementitious Materials. Deutsche Gesellschaft for Zerst-rungsfreie Pr-fung e.V. Stuttgart, Germany: The German Society for Non-Destructive Testing; 2006. p. 1–5. BB102-CD, Lecture 34.
[104] Rydén N, Dahlen U, Lindh P, Jakobsson A. Impact non-linear reverberation spectroscopy applied to non-destructive testing of building materials. J Acoust Soc Am. 2016;140:3327.
[105] Fowler CMR. The Solid Earth. An introduction to global geophysics. Cambridge, UK: Cambridge University Press; 2005.
[106] Lindh P, Lemenkova P. Dynamics of strength gain in sandy soil stabilised with mixed binders evaluated by elastic P-waves during compressive loading. Materials. 2022;15(21).
[107] Mavko G, Mukerji T, Dvorkin J. The rock physics handbook. Cambridge, UK: University Press; 2003.
[108] SIS. Methods of testing cement - Part 1: Determination of strength; 2016. Swedish Standard SS-EN 196-1:2016. Article no. STD-8020324. Available from: https://www.sis.se/en/produkter/construction-materials-and-building/construction-materials/cement-gypsum-lime-mortar/ssen19612016/.
[109] SIS. Methods of testing cement - Part 3: Determination of setting times and soundness; 2016. Swedish Standard SS-EN 196-3:2016. Available from: https://www.sis.se/en/produkter/construction-materials-and-building/construction-materials/cement-gypsum-lime-mortar/ssen19632016/.
[110] Roussel N, LeRoy R. The Marsh cone: a test or a rheological apparatus? Cement Concrete Res. 2005;35(5):823–30.
[111] Banfill PFG. The rheology of fresh mortar. Maga Concr Res. 1991;43(154):13–21.
[112] Ferraris CF, Obla KH, Hill R. The influence of mineral admixtures on the rheology of cement paste and concrete. Cem Concr Res. 2001;31(2):245–55.